BOLETIN DE LA SOCIEDAD ESPAÑOLA DE
Cerámica y Vidrio
A R T I C U L O

Synthesis and electrical properties of the pyrochlore-type $Gd_{2-y}La_yZr_2O_7$ solid solution

J. A. DÍAZ-GUILLÉN[1], M. R. DÍAZ-GUILLÉN [1], K. P. PADMASREE[1], J. M. ALMANZA[1], A. F. FUENTES[1], J. SANTAMARÍA[2], C. LEÓN[2].

[1]Cinvestav Saltillo, Apartado Postal 663, 25000-Saltillo, Coahuila, Mexico
[2]GFMC, Departamento de Física Aplicada III, Facultad de Física, Universidad Complutense de Madrid, 28040-Madrid, Spain

Different compositions in the pyrochlore-type $Gd_{2-y}La_yZr_2O_7$ solid solution ($0 \le y \le 1$) were prepared at room-temperature by mechanically milling stoichiometric mixtures of the corresponding oxides. Irrespective of their lanthanum content, as-prepared powder samples consist of single-phase anion deficient fluorite materials, although long-range ordering of cations and anion vacancies characteristic of pyrochlores was observed in all cases after firing the samples at 1500°C. Interestingly, activation energy for oxygen migration in the series decreases as La-content increases, from 1.13 eV for $Gd_2Zr_2O_7$ to 0.81 eV for $GdLaZr_2O_7$, whereas ionic conductivity was found to be almost La-content independent, at least for $y \le 0.8$ at T = 500°C and $y \le 0.4$ at T = 800°C. These results are explained in terms of weaker ion-ion interactions in better ordered structures (i.e., as La-content increases) and highlight the importance of structural ordering/disordering in determining the dynamics of mobile oxygen ions.

Keywords: Pyrochlores; mechanical milling; zirconates; SOFCs; lanthanum.

Síntesis y propiedades eléctricas de la solución sólida $Gd_{2-y}La_yZr_2O_7$ con estructura de tipo pirocloro

Partiendo de mezclas estequiométricas de los óxidos correspondientes, se prepararon por molienda mecánica y a temperatura ambiente diferentes composiciones en la solución sólida $Gd_{2-y}La_yZr_2O_7$ ($0 \le y \le 1$) con estructura de tipo pirocloro y conductora de iones oxígeno. Independientemente del contenido de lantano, los polvos extraídos del molino presentaron difractogramas similares al de una fluorita no estequiométrica aunque en todos los casos, el tratamiento térmico a 1500°C indujo la aparición del ordenamiento de largo alcance de cationes y vacancias aniónicas característico de pirocloros. La energía de activación para el proceso de migración de iones oxígeno en la serie disminuye a medida que se incrementa el contenido de lantano, desde 1.13 eV de $Gd_2Zr_2O_7$ hasta 0.81 eV de $GdLaZr_2O_7$, mientras que la conductividad resultó ser prácticamente independiente del mismo hasta $y \le 0.8$ para T = 500°C e $y \le 0.4$ para T = 800°C. Estos resultados se explican en términos de una menor interacción entre portadores de carga en las estructuras más ordenadas (a medida que se incrementa el contenido de La) y subraya la influencia del orden/desorden estructural en la dinámica de iones móviles.

Palabras clave: Pirocloros; molienda mecánica; circonatos; pilas de combustible cerámicas; lantano.

1. INTRODUCTION

Working Solid Oxide Fuel Cells (SOFC's) are currently based on a combination of a Sr-doped $LaMnO_3$ (LSM) cathode, the conventional 8YSZ solid electrolyte (yttria-stabilized zirconia with 8 mol% Y_2O_3) and a Ni-YSZ cermet anode. Unfortunately, cell performance is significantly affected by solid state reactions between components which have been frequently observed during co-sintering or even during long-term operation. Thus, the formation of insulating $La_2Zr_2O_7$ and $SrZrO_3$ zirconates have been detected at the cathode/electrolyte interface after firing at temperatures as low as 1100°C. Although different strategies have been suggested in literature to overcome this problem while maintaining the 8YSZ electrolyte (1, 2), alternative ceramic oxide-ion conductors have been also proposed for high temperature SOFC's. Amongst them, pyrochlore oxides $A_2B_2O(1)_6O(2)$, have drawn a great deal of attention because of their chemical and structural flexibility. Since electroneutrality in these oxides can be achieved by a large combination of cation species A and B with different oxidation states, their electrical behavior varies widely. Thus, some pyrochlores behave as insulators or semiconductors and some others show high ionic, electronic or mixed conductivity which makes them ideally suited for the design and construction of monolithic fuel cells (3). Although they might be considered as "ordered" defect fluorites with twice the cell constant, activation energies for oxygen diffusion found in pyrochlores are in general lower than those observed in non-stoichiometric fluorites. Thus, activation energy for migration is considerably lower in the partially ordered pyrochlore-type gadolinium zirconate (P-$Gd_2Zr_2O_7$) than in its fully disordered analogue, the fluorite-type F-$Gd_2Zr_2O_7$ which is obtained by annealing the first above 1500ºC and quenching the powders to room-temperature (4). In consequence, ionic conductivity is higher in P-$Gd_2Zr_2O_7$ than in F-$Gd_2Zr_2O_7$ and comparable to that shown by stabilized zirconias. Oxygen

ions in "ideal" or "ordered" pyrochlores fully occupy two crystallographically different sites, the 48f and 8a according to Wyckoff notation, leaving another possible position, the 8b, systematically empty. Using computing simulation techniques, van Dijk et al. (4) proposed for pyrochlores an oxygen diffusion mechanism consisting of sequential 48*f* to 48*f* ion jumps, along the <100> and <110> directions. Therefore, vacancies must be created by disordering the anion sublattice before migration can take place with the three anion positions, 48*f*, 8*a* and 8*b*, ending up partially occupied. That is, whereas "ideal" pyrochlores render very low conductivity values because of oxygen vacancy ordering, their disordered or "defect" analogues are good ionic conductors. Interestingly enough, structural disorder in pyrochlores might be manipulated in systems of solid solutions by using the appropriate substitutions on the A and B sites, with optimal conductivity obtained for partially ordered phases where ionic interactions penalizing ion migration can be minimized. In this work we analyze the electrical properties of mixed Gd/La pyrochlore-type zirconates of general formula $Gd_{2-y}La_yZr_2O_7$ as a first step towards considering them as a possible alternative to the 8YSZ electrolyte in SOFC's combined with LSM perovskite cathodes. This solid solution is currently under consideration as a promising candidate for ceramic thermal barrier coatings (TBCs) due to its low thermal conductivity (5) although to the best of our knowledge, no data have been previously published on the ionic conductivity of this system. As disorder enthalpies are estimated to be much higher in the lanthanum zirconate than in its gadolinium analogue (6), increasing La-content should produce better-ordered pyrochlores and it would be interesting to analyze its effect on the dynamics of mobile oxygen ions and consequently, on the ionic conductivity of the series. As $La_2Zr_2O_7$ has been shown to be a mixed conductor at high temperature and high oxygen pressures (7, 8), we have limited our study to $Gd_{2-y}La_yZr_2O_7$ samples with $y \leq 1$, where electronic contribution should be negligible and dc conductivity purely ionic.

2. EXPERIMENTAL

Several compositions of general formula $Gd_{2-y}La_yZr_2O_7$ and different Gd/La ratios were prepared by mechanical milling. Stoichiometric mixtures of high-purity (>99+%) La_2O_3, Gd_2O_3 and ZrO_2 were placed in zirconia containers together with 20 mm diameter zirconia balls as grinding media (balls to powder mass ratio = 10:1). Dry mechanical milling was carried out in air in a planetary ball mill by using a rotating disc speed of 350 rpm. Prior to mixing, rare-earth sesquioxides were fired overnight at 900°C in order to decompose hydroxides, carbonates and oxycarbonates present. Phase evolution on milling was periodically analyzed by using X-ray powder diffraction (XRD) in a Philips X'pert diffractometer using Ni-filtered CuK_α radiation (λ = 1.5418 Å). The mechanically induced chemical reaction was considered completed after 27 hours, when no traces of the starting reagents were observed by this technique. Electrical properties were measured between 200 and 800ºC, on pellets (10 mm diameter and ~1 mm thickness) obtained by uniaxial pressing of the fine powders prepared by mechanical milling. To increase their mechanical strength and obtain dense samples, pellets were fired at 1500°C for 6 hours (heating and cooling rates 2°C/min). AC impedance measurements were carried out in air by using a Solartron 1260 Frequency Response Analyzer over the 100 Hz to 1 MHz frequency range. Electrodes for impedance spectroscopy were made from platinum paste after firing in air at 800ºC to eliminate organic components and harden the residue.

3. RESULTS AND DISCUSSION

3.1. Synthesis and structural characterization

Figure 1 shows the XRD patterns of three selected Gd_2O_3:La_2O_3:ZrO_2 mixtures (molar ratio = 1:0:2, 0.9:0.1:2 and 0.6:0.4:2 respectively), after milling them as described above. Irrespective of their La-content, milled powders present simple and very similar XRD patterns which resemble the characteristic of a fluorite-type compound. As the pyrochlore crystal structure might be considered as a superstructure of an anion-deficient fluorite-like atomic arrangement, its X-ray diffraction pattern may be regarded as composed by two set of reflections, one of strong intensity containing all the characteristic reflections of the underlying fluorite-type subcell and a second set of reflections characterizing the long-range ordering of cations and anion vacancies of pyrochlores. Interestingly, the intensities of the latter depend on factors such as the degree of ordering, the differences in the average scattering factors of the elements involved or the distribution of oxygen vacancies (9). As no evidence of this second set are observed in samples prepared by milling, we might assume that this powder processing method favors the formation of highly defective samples with an average crystal structure similar to that of anion deficient fluorites. According to literature, pyrochlore formation in zirconates and titanates at atmospheric pressure is basically controlled by the ionic radius ratio, R_A/R_B; thus, the pyrochlore stability field expands from 1.46 to 1.78, limiting values corresponding to $Gd_2Zr_2O_7$ and $Sm_2Ti_2O_7$ respectively (10). Anion deficient fluorites would be then obtained when $R_A/R_B < 1.46$. However, mechanical milling allows the room-temperature preparation of single phase

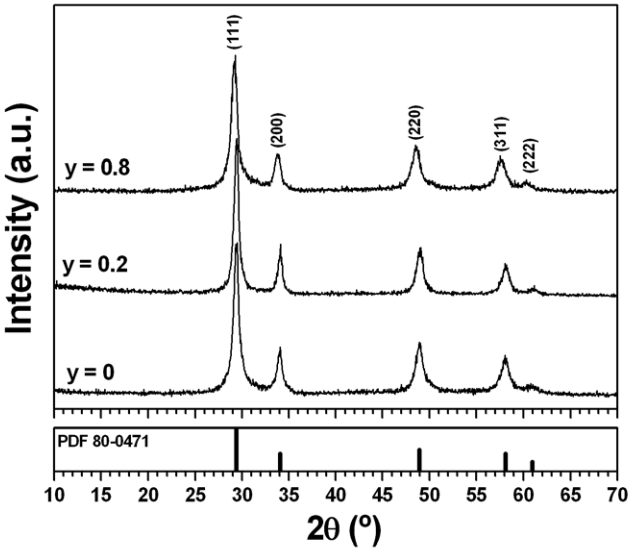

Fig. 1- XRD patterns obtained for three selected Gd_2O_3:La_2O_3:ZrO_2 compositions after milling at room-temperature for 27 hrs; "y" values shown are referred to the general formula $Gd_{2-y}La_yZr_2O_7$. As a reference, the reported XRD pattern of F-$Gd_2Zr_2O_7$ is shown at the bottom; numbers in parenthesis are the Miller indexes of each reflection.

metastable fluorite-type $Gd_{2-y}La_yZr_2O_7$ powders despite of R_A/R_B values well above 1.46 (i.e., 1.54 for $GdLaZr_2O_7$). Increasing shift towards low angle (2θ) as the La-content increases in figure 1, is consistent with an increase in cell size (R_{Gd}(VIII) = 1.053 Å vs. R_{La}(VIII) = 1.16 Å (11)) and proves the existence of a mechanically induced chemical reaction on milling these powder mixtures. Figure 2 shows the XRD patterns collected for the same samples after firing them 6 hours at 1500ºC and slow cooling to room-temperature; superstructure reflections characterizing the pyrochlore crystal structure (i.e. the (111) and (331) peaks at ≈ 15 and 37° (2θ) respectively), are now evident. Therefore, post-milling thermal treatments of the as-prepared mixed zirconates at high temperature facilitate the long-range ordering of cations and anion vacancies characteristic of pyrochlores. No additional reflections belonging to third phases were ever observed.

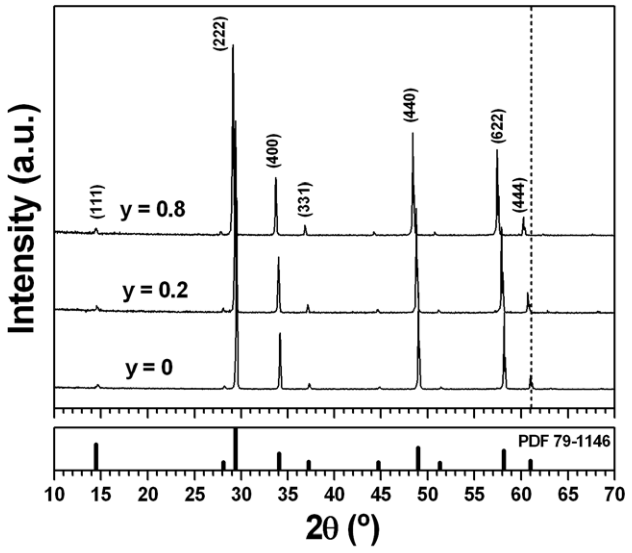

Fig. 2- XRD patterns collected for the same powder samples shown in figure 1, after firing them 6 hrs at 1500°C and slow cooling to room-temperature. As a reference, the reported XRD pattern of P-$Gd_2Zr_2O_7$ is shown at the bottom whereas numbers in parenthesis are the Miller indexes of the main reflections of the pyrochlore-type crystal structure. Vertical dashed line is a guide to the eye and is only shown to emphasize the increase in cell size as lanthanum-content increases.

3.2. Electrical properties

Figure 3 shows the frequency and temperature dependence of the real part of the electrical conductivity, σ′(ω), for the pyrochlore-type $Gd_{1.2}La_{0.8}Zr_2O_7$ sample selected as representative of the series. Similar conductivity plots were obtained for all samples analyzed in this work. As this figure shows, the frequency dependence of conductivity at low temperatures may be well described by the so-called Jonscher empirical expression (12), $\sigma'(\omega) \propto \omega^n$, consistent with a power law-type dependence at high frequencies followed by a frequency-independent conductivity plateau associated to the dc conductivity regime, σ_{dc}. This behavior constitutes the main feature of the so-called "universal dielectric response" and has been linked with the existence of cooperative effects in the dynamics of hopping ions (13). The value of the fractional exponent n ($0 \le n < 1$) is determined by the strength of the ion-ion interactions in the ionic hopping process; i.e. in the absence of interactions among mobile ions (completely independent and random ion hopping), the exponent n would be 0. The decrease in conductivity clearly visible at low frequencies between 250 and 500°C, is caused by blocking effects at grain boundaries whereas that observed at 800°C is due to blocking at the electrodes.

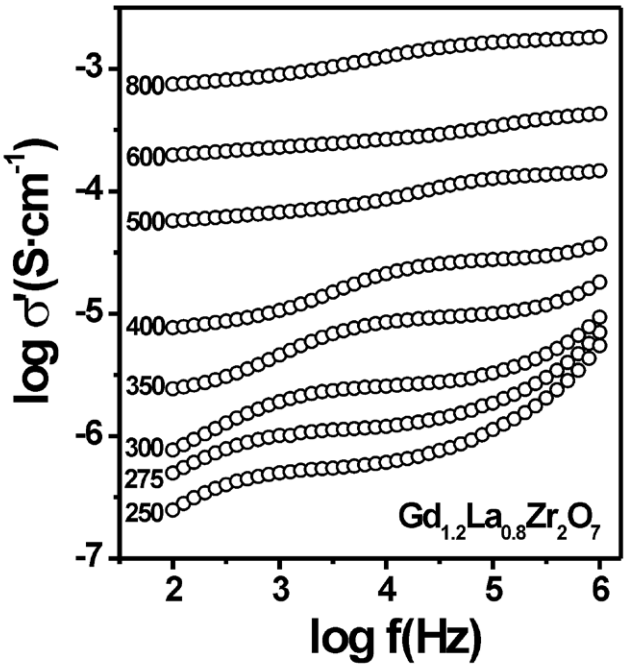

Fig. 3- Real part of the conductivity vs frequency at several temperatures (°C) for the $Gd_{1.2}La_{0.8}Zr_2O_7$ sample showing a power-law behavior at high frequencies and low temperatures.

Figure 4 shows the real part of the dielectric permittivity as a function of frequency and temperature for the same composition. Again, blocking effects at grain boundaries and electrodes are observed and shift to lower frequencies with

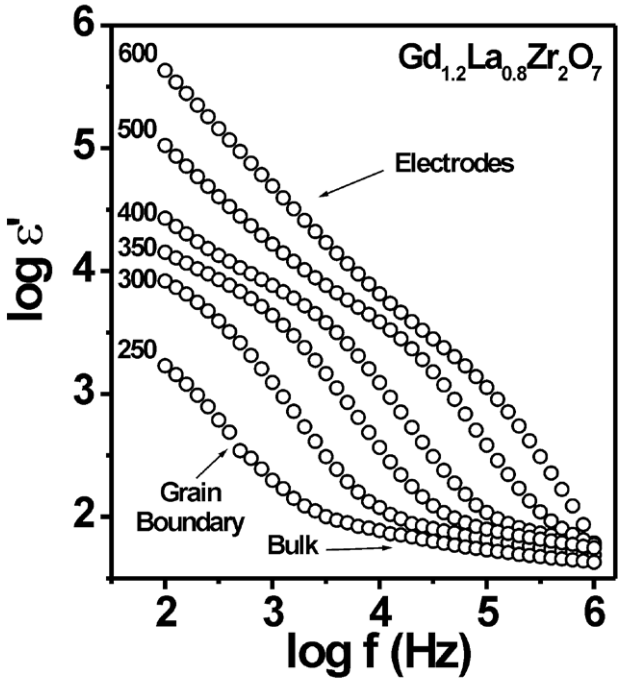

Fig. 4- Frequency dependence of the real part of permittivity of $Gd_{1.2}La_{0.8}Zr_2O_7$, at selected temperatures (°C).

decreasing temperature. The value of the high frequency permittivity, $\varepsilon_\infty = 35 \pm 3$, is found to be almost independent of temperature and La-content for the whole series. Grain boundary resistance is also evident in figure 5 which shows a complex impedance plot obtained at 350°C for the same $Gd_{1.2}La_{0.8}Zr_2O_7$ composition. Two main features can be observed in this figure: an incomplete arc at low frequencies with capacitance values typical of grain boundary contributions ($C_{gb} = 1.6 \cdot 10^{-9}$ F·cm^{-1}) and another one at high frequencies associated with the bulk contribution ($C_g = 6.2 \cdot 10^{-12}$ F·cm^{-1}). Either from the conductivity value at the high-frequency plateau in figure 3 or from the semicircles shown in figure 5, the bulk dc conductivity was easily obtained from the experimental data for the whole series.

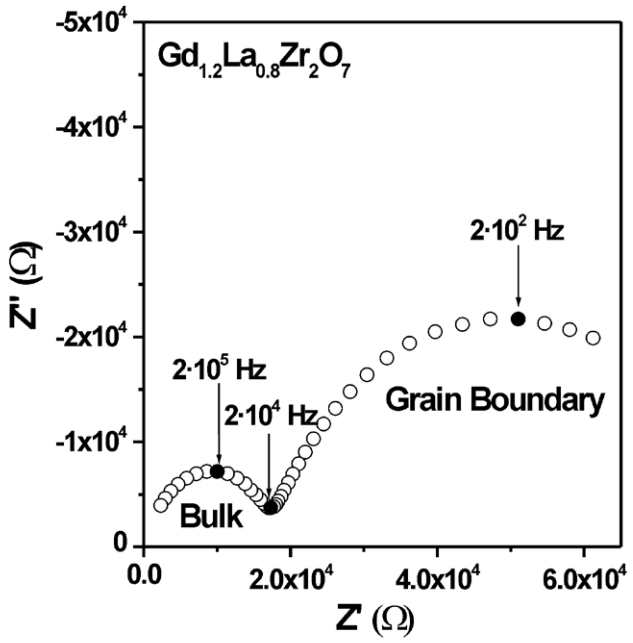

Fig. 5- Complex impedance plot obtained at 350°C for $Gd_{1.2}La_{0.8}Zr_2O_7$. Filled circles represent selected frequencies in Hertz.

The temperature dependence of the bulk dc conductivity for the samples under study was analyzed by using an Arrhenius-type law of the form: $\sigma_{dc} \cdot T = (\sigma_0) \exp(-E_{dc}/k_B T)$, where σ_0 is the pre-exponential factor which is related to the effective number of mobile oxygen ions and E_{dc} denotes the activation energy for the ion conduction process. Figure 6 shows such representations where the lines are least squares best fit to an Arrhenius law confirming that ionic diffusion in the series is thermally activated. Activation energies and pre-exponential factors for the whole series calculated from the slope and intercept of these linear fits, respectively, are presented in Table 1 and show a marked decrease as lanthanum content increases. Thus, replacing Gd in $Gd_2Zr_2O_7$ by a larger cation as La implies increasing ordering (the pre-exponential factor decreases and therefore, the number of mobile species) but it also decreases the activation energy needed for the anion vacancies to migrate which as figure 7 shows, results in dc conductivity remaining almost La-content independent, at least for $y \leq 0.8$ at T = 500°C and $y \leq 0.4$ at T = 800°C.

As cooperative effects in oxygen hopping dynamics have been shown to be a key factor in determining conductivity in a similar system (14, 15), we will proceed now examining the influence of Gd substitution in the ion-ion correlations of this solid solution.

TABLE I. ACTIVATION ENERGIES, PRE-EXPONENTIAL FACTORS AND VALUES OF N FOR THE $GD_{2-Y}LA_YZR_2O_7$ SYSTEM

La content (y in $Gd_{2-y}La_yZr_2O_7$)	Pre-exponential factor (S·K·cm^{-1})	E_{dc} (eV)	n
0	$1.8 \cdot 10^6$	1.13	0.52
0.2	$1.9 \cdot 10^6$	1.10	0.52
0.3	$1.5 \cdot 10^6$	1.05	0.51
0.4	$6.4 \cdot 10^5$	1.00	0.49
0.8	$3.3 \cdot 10^4$	0.85	0.46
1	$6 \cdot 10^3$	0.81	0.44

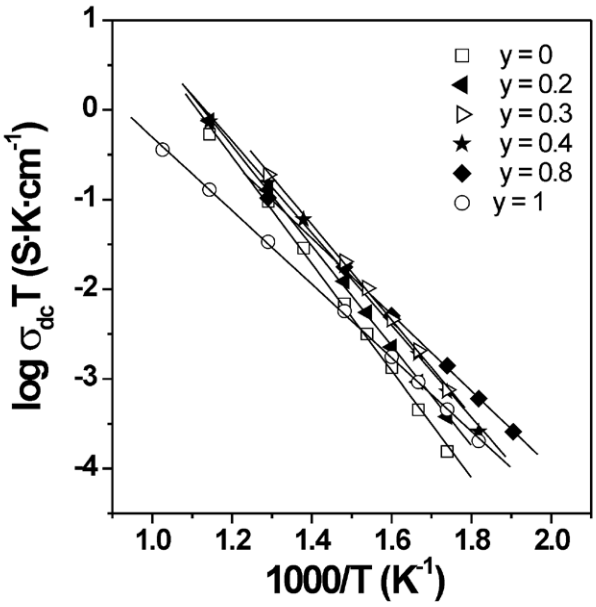

Fig. 6- Arrhenius plots of the bulk dc conductivity for the $Gd_{2-y}La_yZr_2O_7$ series ($0 \leq y \leq 1$) Solid lines are the least squares best fit to the data.

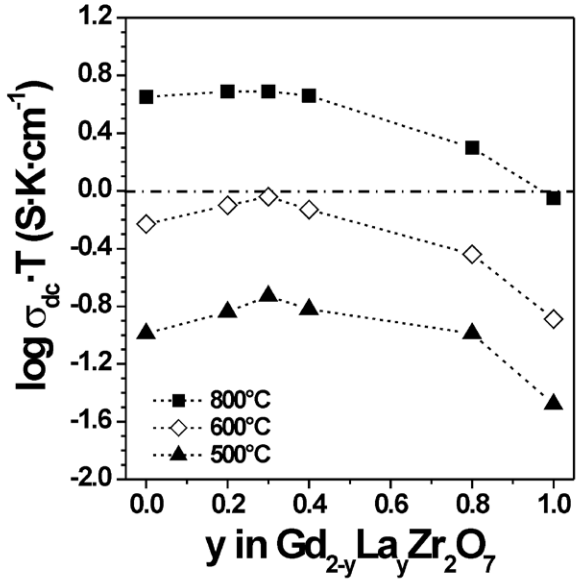

Fig. 7- dc conductivity vs. La content for the title solid solution at three selected temperatures

Electrical relaxation data may be also described in terms of the electric modulus which is the inverse of the dielectric permittivity and thus, is directly related to the conductivity through the equation:

$$M^*(\omega) = 1/\varepsilon^*(\omega) = j\omega\varepsilon_0/\sigma^*(\omega) \quad [1]$$

The electric modulus can be expressed then by the Fourier transform of the time derivative

$$M^*(\omega) = \frac{1}{\varepsilon_\infty}\left[1 - \int_0^\infty \left(-\frac{d\Phi}{dt}\right)e^{-j\omega t}dt\right] \quad [2]$$

of the so-called Kohlrausch-Williams-Watts (KWW) relaxation function of the form (16):

$$\Phi(t) = \exp(-(t/\tau)^{1-n}), \qquad 0 < (1-n) \le 1. \quad [3]$$

where ε_∞ is the dielectric permittivity at high frequencies and τ the characteristic relaxation time of the ion-hopping process which is thermally activated with the same activation energy of the dc conductivity. Correspondingly, the time dependence indicated in equation [3] is reflected by the spectral shape of the imaginary part of the electric modulus as an asymmetric relaxation peak at a characteristic frequency $\omega_p \approx \tau^{-1}$, which increases with increasing temperature. The fractional exponent n defines the power law dependence of the M''(ω) above the peak frequency as ω^{n-1}, and consequently the power law dependence of the real part of the conductivity ($\sigma'(\omega) \propto \omega^n$) at high frequencies. Thus, as mentioned before, the value of n is a measure of the departure from the pure exponential or Debye behavior expected for uncorrelated ion hopping. Figure 8 shows the frequency dependence of the real and imaginary parts of the electric modulus at two selected temperatures for the same $Gd_{1.2}La_{0.8}Zr_2O_7$ powder sample. The figure also shows best fits according to equations [2] and [3], in excellent agreement with experimental data and from which,

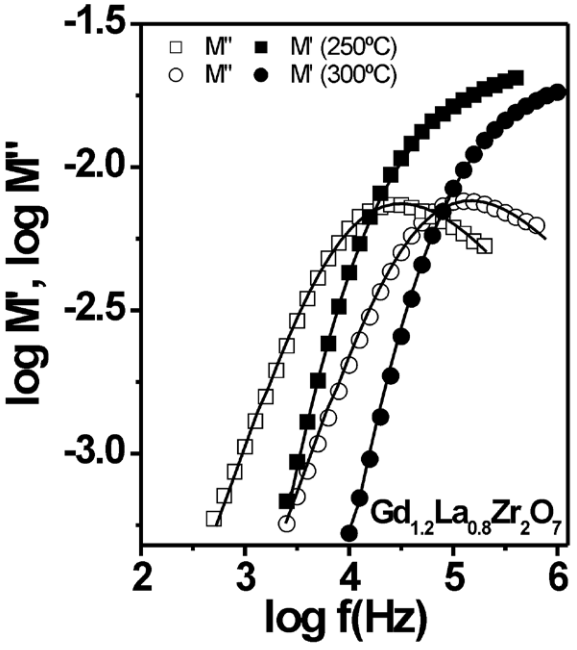

Fig. 8- Frequency dependence of the real (solid symbols) and imaginary parts (open symbols) of $Gd_{1.2}La_{0.8}Zr_2O_7$ electric modulus at two selected temperatures. Solid lines are best fits according to a KWW relaxation function.

the values of the exponent n were obtained and observed to be temperature independent for each sample (at least for T ≤ 325°C; at temperatures higher than that, the peak maxima typically shift out of the experimental frequency window used in this work). As shown in Table 1, both the pre-exponential factor and the value of the exponent n in the series were found to show a similar trend and decrease with increasing lanthanum content (n changes from 0.52 ± 0.01 for $Gd_2Zr_2O_7$ to 0.44 ± 0.01 for $GdLaZr_2O_7$). Thus, σ_0 remain almost constant for the first part of the solid solution (y ≤ 0.4) suggesting that this level of La incorporation does not have much influence on the degree of structural ordering/disordering of P-$Gd_2Zr_2O_7$. Accordingly, the value n in this group of samples is nearly constant within experimental errors. However, increasing size mismatch between cations at the A and B site (y > 0.4) generates better ordered samples as revealed by the σ_0 value which decreases substantially in this compositional range (decreasing number of mobile oxygens). This fact also shows in the value of n which decreases significantly when 0.4 < y ≤ 1. These results are consistent with the previous finding of the latter being related to the degree of structural order/disorder in ionically conducting pyrochlore oxides (14, 15). In the present case, a more ordered structure is induced by increasing lanthanum content and n decreases accordingly.

Different models have been proposed to analyze electrical relaxation data in ionic conductors (13, 17, 18) which take into account the existence of cooperative effects among mobile ions in the diffusion process. Interestingly, our results of a concomitant decrease of the activation energy E_{dc} for the dc conductivity and of the value of n, with increasing ordering (see Table 1), can be rationalized in terms of the Coupling Model (CM) (13, 17, 19, 20). The CM starts with the consideration of independent hops of ions to vacant adjacent sites with exponential correlation function, , and relaxation time τ_0. Such independent hops cannot occur for all ions at the same time because of ion-ion interactions and correlations. The result of ion-ion interactions is the slowing down of the relaxation rate at times longer than t_c of the order of 2 ps, changing the correlation function from a pure exponential to a KWW function, $\Phi(t) = \exp(-(t/\tau)^{1-n})$, wherein the value of the fractional exponent n is a measure of the cooperative effects. A major result from the CM is that the effective relaxation time τ is related to τ_0 by

$$\tau = [t_c^{-n}\tau_o]^{1/(1-n)} \quad [4]$$

For ions vibrating in their cages and hopping to neighboring sites through barriers of energy E_a, the relaxation time for independent ion hopping is $\tau_o(T) = \tau_\infty \exp(E_a/kT)$. The reciprocal of τ_∞ is the attempt frequency of ions. It follows from equation [4] that the activation energy for the dc conductivity or τ will be larger than the energy barrier and given by the relation.

$$E_{dc} = E_a/(1-n) \quad [5]$$

The increase of ion-ion interaction leads to a higher degree of cooperativity in the ion hopping process which corresponds to a higher value of n and, consequently, to higher activation energy for long-range ionic transport due to the energy penalty that ion-ion interactions impose on the ionic diffusion process. In fact, the activation energy E_a for the barrier that oxygen ions must overcome to hop (independently) between

neighboring vacant sites in the $Gd_{2-y}La_yZr_2O_7$ series ($0 \le y \le 1$), can thus be estimated according to equation [5] by using the experimental values obtained for E_{dc} and n. A value $E_a = 0.50 \pm 0.04$ eV is found, independent of La content within experimental error (figure 9). A lower La-content leads to a higher degree of structural disorder, where enhanced ion-ion interactions are expected, and consequently also to higher values of the exponent n according to the CM. The more disordered structure fosters ion-ion correlations, and lead to an increase of the energy penalty that these correlations impose on long-range or dc ionic conductivity. This explains the larger difference found between E_{dc} and E_a (larger value of n), the lower the La-content for the $Gd_{2-y}La_yZr_2O_7$ series (see figure 9).

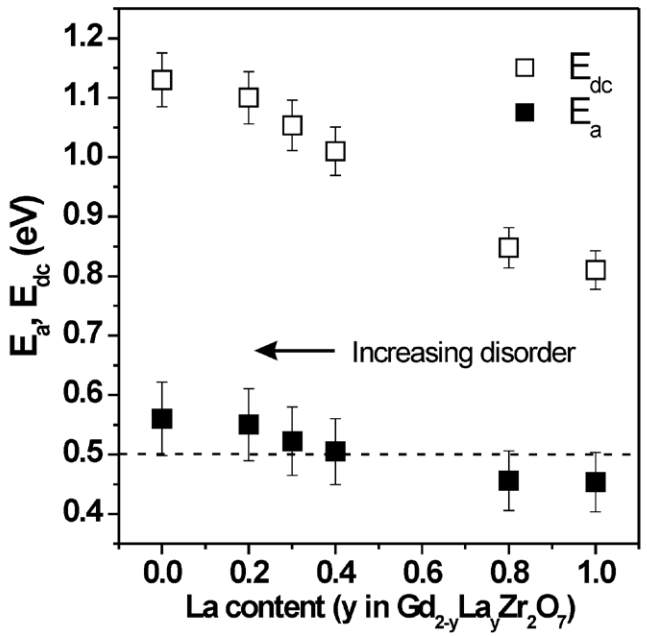

Fig. 9- Values obtained for the activation energy E_{dc} (□) and the energy barrier $E_a = (1 - n)\ E_{dc}$ (■) as a function of lanthanum content. The dashed line represents the average E_a value.

4. CONCLUSIONS

We have shown that compositions in the $Gd_{2-y}La_yZr_2O_7$ solid solution having different Gd/La ratios can be easily prepared at room-temperature, by mechanically milling stoichiometric mixtures of the corresponding elemental oxides. Although as-prepared powder samples show XRD patterns similar to those characteristic of anion deficient fluorites, post-milling thermal treatments at 1500°C give rise to a partial redistribution of cations and oxygen vacancies and the appearance of the long-range atomic ordering characteristic of pyrochlores. Despite of a decreasing number of mobile oxygen vacancies by increasing La-content (increasing structural ordering), we have found that ionic conductivity in the series is almost La content independent for $y \le 0.8$ at T = 500°C and $y \le 0.4$ at T = 800°C. This fact is explained by a systematic decrease in the activation energy for the dc ionic conductivity with increasing ordering, that is with increasing La content. From the analysis of electrical conductivity relaxation data in terms of Ngai's Coupling Model, we conclude this behavior is due to the enhancement of ion-ion interactions promoted by the more disordered structure in samples with higher Gd content.

ACKNOWLEDGMENTS

This work has been carried out with the financial support of Mexican Conacyt (Grant SEP-2003-C02-44075) and Spanish MCYT (MAT2004-3070-C05).

REFERENCES

1. H. Yokokawa, N. Sakai, T. Kawada, M. Dokiya, Thermodynamic analysis of reaction profiles between lanthanum metal oxides ($LaMO_3$, M = nickel, cobalt, or manganese) and zirconium oxide, J. Electrochem. Soc. 138, 2719-2727 (1991).
2. Y. Takeda, Y. Sakaki, H.-Y. Tu, M. B. Phillipps, N. Imanishi, O. Yamamoto, Perovskite oxides for the cathode in solid oxide fuel cells, Electrochemistry 68, 764-770 (2000).
3. H. L. Tuller, Ionic and mixed conductors: materials design and optimization, in eds. F. W. Poulsen, N. Bonanos, S. Linderoth, M. Mogensen, B. Zachau-Chistiansen, High temperature electrochemistry: ceramics and metals, Proceedings 17th Riso International Symposium on Materials Science, Riso National Laboratory, Roskilde, Denmark, pp. 139-153 (1996).
4. M. P. van Dijk, A. J. Burggraaf, A. N. Cormack, C. R. A. Catlow, Defect structures and migration mechanisms in oxide pyrochlores, Solid State Ion. 17, 159-167 (1985).
5. C. L. Wang, W. Pan, Q. Xu, Y. X. Qin, J. D. Wang, Z. X. Qu, M. H. Fang, Effect of point defects on the thermal transport properties of $(La_xGd_{1-x})_2Zr_2O_7$: experimental and theoretical model, Phys. Rev. B 74, 144109 (2006).
6. L. Minervini, R. W. Grimes, K. E. Sickafus, Disorder in pyrochlore oxides, J. Am. Ceram. Soc. 83, 1873-1878 (2000).
7. T. H. Etsell, S. N. Flengas, The electrical properties of solid oxide electrolytes, Chem. Rev. 70, 339-76 (1970).
8. J. A. Labrincha, J. R. Frade, F. M. B. Marques, $La_2Zr_2O_7$ formed at ceramic electrode/YSZ contacts, J. Mater. Sci. 28, 3809-3813 (1993).
9. C. Heremans, B. J. Wuensch, J. K. Stalick, E. Prince, Fast-ion conducting $Y_2(Zr_yTi_{1-y})_2O_7$ pyrochlores: neutron Rietveld analysis of disorder induced by Zr substitution, J. Solid St. Chem. 117, 108-21 (1995).
10. M. A. Subramanian, G. Aravamudan, G. V. Subba Rao, Oxide pyrochlore-A review, Prog. Solid St. Chem. 15, 55-143 (1985).
11. R. D. Shannon, Revised effective ionic radii and systematic studies of interatomic distances in halides and chalcogenides, Acta Cryst. A32, 751-767 (1975).
12. A. K. Jonscher, Dielectric Relaxation in Solids, Chelsea Dielectric Press, London, 1984.
13. K. L. Ngai, R. W. Rendell, Basic physics of the coupling model: direct experimental evidences, ACS Symposium Series 676, 45-66 (1997).
14. K. J. Moreno, G. Mendoza-Suárez, A. F. Fuentes, J. García-Barriocanal, C. León, J. Santamaría, Cooperative oxygen dynamics in $Gd_2Ti_{2-y}Zr_yO_7$, Phys. Rev. B 71, 132301 (2005).
15. K. J. Moreno, A. F. Fuentes, M. Maczka, J. Hanuza, U. Amador, J. Santamaría, C. León, Influence of thermally induced oxygen order on mobile ion dynamics in $Gd_2Ti_{0.65}Zr_{0.35}O_7$, Phys. Rev. B 75, 184303 (2007).
16. P. B. Macedo, C. T. Moynihan, R. Bose, Role of ionic diffusion in polarization in vitreous ionic conductors, Phys. Chem. Glasses 13, 171-179 (1972).
17. K. L. Ngai, C. León, Recent advances in relating macroscopic electrical relaxation data to microscopic movements of the ions in ionically conducting materials, Solid State Ion. 125 81-90 (1999).
18. K. Funke, R. D. Banhatti, C. Cramer, Correlated ionic hopping processes in crystalline and glassy electrolytes resulting in MIGRATION-type and nearly constant-loss-type conductivities, Phys. Chem. Chem. Phys. 7, 157-165 (2005).
19. K. L. Ngai, C. León, Cage decay, near constant loss and crossover to cooperative ion motion in ionic conductors: insight from experimental data, Phys. Rev. B 66, 064308 (2002).
20. K. L. Ngai, C. León, A quantitative explanation of the difference between nuclear spin relaxation and ionic conductivity relaxation in superionic glasses, J. Non-Cryst. Solids 315, 124-133 (2003).

Recibido: 31.07.07
Aceptado: 20.12.07